Journal of Mechanical Engineering and Sciences
ISSN (Print): 2289-4659; e-ISSN: 2231-8380
Volume 13, Issue 3, pp. 5424-5440, September 2019

DOI: https://doi.org/10.15282/jmes.13.3.2019.14.0440

On the preparation of EPDM-*g*-MAH compatibilizer via melt-blending method

J. A. Razak[1], N. Mohamad[1], M. A. Mahamood[1], R. Jaafar[1], I. S. Othman[1], M. M. Ismail[2], L. K. Tee[3], R. Junid[4] and Z. Mustafa[1]

[1]Fakulti Kejuruteraan Pembuatan, Universiti Teknikal Malaysia Melaka, Hang Tuah Jaya, 76100, Durian Tunggal, Melaka, Malaysia,
[*]Email: jeefferie@utem.edu.my
Phone: +60126087651; Fax: +6062701047
[2]Fakulti Kejuruteraan Elektronik & Kejuruteraan Komputer, Universiti Teknikal Malaysia Melaka, Hang Tuah Jaya, 76100, Durian Tunggal, Melaka, Malaysia,
[3]Fakulti Teknologi Kejuruteraan Mekanikal & Pembuatan, Universiti Teknikal Malaysia Melaka, Hang Tuah Jaya, 76100, Durian Tunggal, Melaka, Malaysia,
[4]Faculty of Mechanical Engineering, Universiti Malaysia Pahang, 26600, Pekan, Pahang, Malaysia

ABSTRACT

This paper presents an experimental investigation to determine the optimum composition of maleic anhydride (MAH) and dicumyl peroxide (DCP) as initiator, for ethylene-propylene-diene-monomer grafted MAH (EPDM-*g*-MAH) compatibilizer preparation, using Response Surface Methodology (RSM) approach. EPDM-*g*-MAH was prepared in the laboratory scale by melt blending method using an internal mixer. For this study, the effects of MAH (2.50 – 7.50 wt.%) and DCP (0.10 – 0.30 wt.%) towards grafting efficiency was determined. Two level full factorial design of experiment (DOE) has applied to establish the relationship between these two independent factors of raw materials. Analysis of variance (ANOVA) and the optimization menu have utilized to decide the raw materials formulation with maximum grafting efficiency. Quantitative analysis based on infrared (IR) spectral intensity supported by ^{1}H-NMR spectral are used to propose for EPDM-*g*-MAH grafting mechanism. Standard calibration curve for quantity ratio plot was exponential with R^2 = 89.19%. It has found that an optimum about 8.52% of MAF grafting efficiency has yielded about DCP factor contributed larger effect at 67.45% of contribution effect. Anhydride stretching of grafted C=O as confirmed by FTIR peak at 1713 cm^{-1} and 1770 – 1792 cm^{-1} has responsible for MAH grafting into EPDM rubber. Based on FTIR, ^{1}H-NMR and 2D-COSY spectral analysis, reaction mechanism for EPDM-*g*-MAH grafting has successfully proposed with two possible termination steps. In overall, this study was significant to introduce the simplest optimum method of laboratory scale EPDM-*g*-MAH compatibilizer using melt blending and DOE approach.

Keywords: EPDM-*g*-MAH grafting; RSM; DOE; standard calibration; IR quantitative analysis.

INTRODUCTION

EPDM is a specialty elastomer for engineering and technology application. This synthetic rubber has synthesized from the polymerization of ethylene and propylene with small amount of non-conjugated diene at about 3 – 9% [1]. EPDM is non-saturated and non-polar due to lower content of –C=C- [2]. The chemical structure of EPDM has illustrated as in the following Figure 1. EPDM not possessed the polar group or any chemical group with higher electron density. This situation complicates the bond between EPDM and other materials. EPDM with higher unsaturation level is more compatible with diene rubber such as natural rubber (NR) to improve their waste, heat, ozone, weather, environment and impact resistance [3].

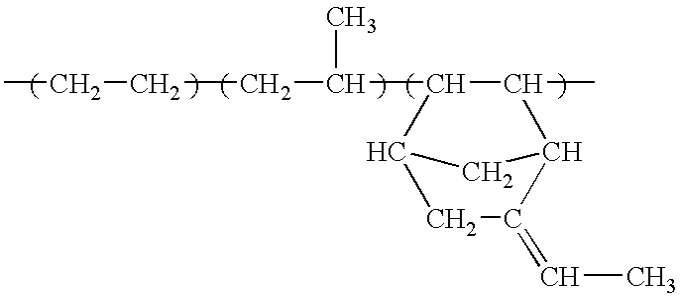

Figure 1. Chemical structure of EPDM rubber [4].

Normally, in the preparation of NR/EPDM blend, the EPDM phase component is relatively critical to consider because of its advantages as impact modifier, resistance enhancer towards heat and chemical and superior ageing properties [5]. However, non-polarity and highly unsaturation behaviour of EPDM are the main cause incompatibility and immiscibility of elastomer blends that involve the presence of EPDM rubber phase. EPDM rubber modification need to perform through copolymer product preparation using simple grafting method to enhance the blend compatibility [6]. The copolymer products obtained used as a compatibilizer for most of rubber blends [7]. This study was to prepare the copolymer of EPDM grafted with MAH (EPDM-g-MAH) by melt blending using a design of experiment approach.

Grafting of EPDM with MAH produces elastomer with local polarity and increasing chemical reactivity [8]. The use of EPDM-*g*-MAH compatibilizer has dual-function acting on an anhydride-polar part, which results in a good affinity to the filler surface, while the polymer that attached gives the compatibilization effects and interaction to the blends [9]. EPDM modifications with MAH, are expected to increase the cross-link density if EPDM phase resulting in higher polarity for uniformity of curative distribution [10].

A recent study involving the preparation of EPDM-*g*-MAH was reported [6, 11-13, 18]. Grigoryeva and Karger-Kocsis (2000) have successfully evaluated the impact of MAH grafted to EPDM by taking into account various preparation factor of compatibilizer such as MAH content, grafting temperature, rotor speed and mixing chamber volume [12]. The same applies to the compatibilizer preparation for poly (butylene succinate) grafted with MAH (PBS-g-MAH) by Phua et al. (2013) [9]. The study suggests that the DCP initiator content is around 1.00 – 1.50 phr without involving the any interaction factor between the studied independent and dependent variables.

Hence, this study took the opportunity to manipulate the DOE approach in analysing the grafting efficiency as response studied and establishing the relationship between the independent and dependent variables [19-24]. In addition, this study also reporting on the utilization of quantitative IR based on FTIR spectral analysis for grafting efficiency determination. At the end, the suggested reaction mechanism was further supported by the ^{1}H-NMR and 2D-COSY analysis.

METHODS AND MATERIALS

Raw Materials

EPDM rubber grade BUNA EP 9650 has supplied by LANXESS, Pittsburgh, USA. Mooney viscosity UML (1+8) at 150°C is around 60±6 MU, with ethylene content of about 54±4 wt.%, ENB content of 6.5±1.1 wt.% with volatile content of ≤ 0.75 wt.%, specific gravity at 0.86 and ash content of ≤ 0.50 wt.%. MAH used was a synthesis grade (95% with maleic acid content ≤ 5.00 %), supplied by Sigma Aldrich Chemie GmbH, Steinheim, Germany. The dicumyl peroxide used is bis (1-methyl-1-phenyl-ethyl) peroxide bis (α-α – dimethyl benzyl peroxide) with molecular weight formula of 270.37, volatile density around 9.30 and steam pressure at 15.40 mmHg. DCP was supplied by Sigma Aldrich, Germany with addition content in the range of 0.10 – 0.50 wt.%.

EPDM-*g*-MAH Compatibilizer Preparation

The EPDM-*g*-MAH compatibilizer has prepared by melt-blending using an internal mixer model Haake Polylab OS Rheodrive 16 with Banbury rotor and fill factor of 0.70. The effects of added DCP and MAH was screened as independent variables for EPDM-g-MAH compatibilizer melt blending by using a two-level full factorial design of experiment. The grafting efficiency as response chosen as dependent variable. The two-level full factorial experiments based on two numerical factor, no categorical factor, involving only one replication with three midpoints and no blocking. Overall, the software has proposed about seven experiment on the preparation of EPDM-g-MAH compatibilizer. The following Table 1 summarized the experimental design used in this study. Table 2 outlined the lower, mid and upper level value of each variable. From the experimental results, the effects of independent variables towards grafting efficiency determined by half-normal plot and the effects list. The factorial model chosen and analysed using the analysis of variance (ANOVA) to test the selected model accuracy. Pure EPDM sample also characterized as a control sample.

Table 1. The selected level for variables.

MAH content (A, wt.%)	DCP content (B, wt.%)
2.50 (-1)	0.10 (-1)
5.00 (0)	0.30 (0)
7.50 (+1)	0.50 (+1)

The grafting process was performed at basic formulation recipe of 100% EPDM (43 grams) with ρ_{EPDM} = 0.802 g/cm^3. At first, the EPDM masticated at 30°C within 10 minutes using the open two-roll mill equipment. Next, the grafting of EPDM-*g*-MAH performed in an internal mixer at fixed processing parameters as suggested by Grigoryeva & Karger-Kocsis, (2000), which are 180°C of blending temperature, 75 rpm of Banbury rotor speed and within 5 minutes of grafting period [12]. Later the grafted EPDM samples were conditioned at 25°C within 24 hours before thin films preparation of EPDM-*g*-MAH samples for *Fourier* transform infra-red (FTIR) analysis.

Table 2. Overall experimental plan and formulation recipes for grafting of EPDM-*g*-MAH compatibilizer preparation

Standard	Test	Block	Factor 1 A:MAH wt.%	Factor 2 B:DCP wt.%	Sample Code	Weight EPDM (grams)	Weight MAH (grams)	Weight DCP (gram)
6	1	1	5.00 (0)	0.30 (0)	EM1	43.00	2.150	0.129
4	2	1	7.50 (+1)	0.50 (+1)	EM2	43.00	3.225	0.215
2	3	1	7.50 (+1)	0.10 (-1)	EM3	43.00	3.225	0.043
5	4	1	5.00 (0)	0.30 (+1)	EM4	43.00	2.150	0.129
1	5	1	2.50 (-1)	0.10 (-1)	EM5	43.00	1.075	0.043
3	6	1	2.50 (-1)	0.50 (0)	EM6	43.00	1.075	0.215
7	7	1	5.00 (0)	0.30 (0)	EM7	43.00	2.150	0.129

FTIR Characterization

For thin film preparation, the EPDM-*g*-MAH samples were hot-pressed at 150°C, within 10 minutes using compressive pressure at 5MPa. Prior to that, five minutes of pre-heat allocated before performing the hot press. The thin films conditioned by immersing it into acetone solution for 30 minutes and drying at 75°C for 24 hours, before the FTIR test has performed. This purification step is important to remove the non-reacted MAH and increase the absorption peak in the same area of the anhydride [14, 15]. The elimination of unreacted MAH has confirmed from the missing of absorption peak at 700 cm^{-1} due to single and double C bonds to MAH [6]. The FTIR spectra is recorded using the Jasco Pro 450 FT/IR-6100(a) equipment, from 2000 to 400 cm-1 wavenumber with a type II laser resolution. A total of 50 times the number of scans on the sample held at vertical position has performed. Later, the obtained IR spectral was then smoothen prior of the quantitative analysis.

NMR Characterization

The nuclear magnetic resonance (NMR) analysis of ^{1}H-NMR and 2D-COSY utilized to confirm the success of MAH grafting into EPDM rubber. It also used as a tool for proposal of EPDM-*g*-MAH reaction mechanism. The NMR test performed by using the spectrometer Bruker Avance 300 MHz with pulse rate of 13.2 µs with transition period of 3.0 seconds. The EPDM-g-MAH film completely immersed in deuterated chloroform ($CDCl_3$) solution and tetramethylsilane (TMS) solution used as standard for internal chemical shift. The two-dimensional correlation spectroscopy (2D-COSY) also recorded with delayed time of 1.62 seconds and scan width of 1930.5 Hz. ^{1}H-NMR and 2D-COSY are able to provide extra information on grafting mechanism based on the presence of protons in the tested grafted polymers [9].

RESULTS AND DISCUSSION

The comparison of FTIIR spectra between pure EPDM rubber, MAH and grafted EPDM-*g*-MAH depicts in the Figure 2. For pure EPDM rubber, the peaks at 2926 and 2856 cm^{-1} were typical of EPDM indicating the presence of saturated hydrocarbon backbone of aliphatic alkyl symmetric or asymmetric C-H stretching vibration. IR spectra for EPDM-*g*-MAH is referred [15, 25, 26]. The absorption bands at the region of 1770 – 1792 cm^{-1}, which attributed to C=O symmetric stretching bonds, were related to successful MAH grafted to the EPDM rubber [27, 28, 29]. The absorption peak at 922 cm^{-1}, confirmed the presence of OH group in EPDM-g-MAH. The missing absorption peak at 1779 to 1780 cm^{-1} that indicate C-O stretching for anhydrides of pure EPDM has confirmed the success of EPDM grafting with MAH [30]. This condition also applies to all IR spectral for grafted EPDM-*g*-MAH as depicted in the Figure 3.

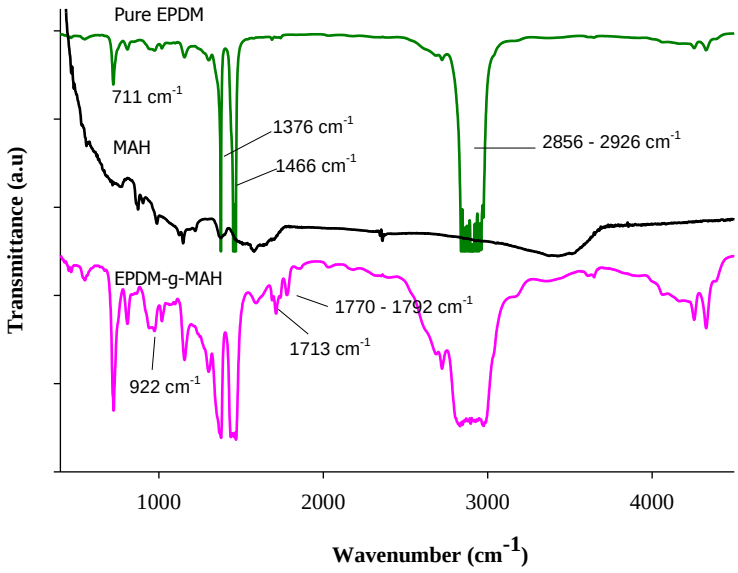

Figure 2. IR spectral comparison between pure EPDM (control sample), MAH and grafted EPDM-*g*-MAH [15].

For quantitative analysis of IR spectral for EPDM-*g*-MAH grafting process, the following Figure 3 shows the selected spectral for comparison. For this purpose, spectral from EM1, EM2 and EM5 have selected. The quantitative analysis of IR spectral performed based on DOE and the application of *Beer-Lambert* equation for grafting efficiency determination for EPDM-*g*-MAH grafting process. Analysis for the entire peaks has made for detecting the anhidrida and selection of internal standard. It was found that there are two important area for anhydride zone, which are peak range at 1860 – 1738 cm^{-1} and 1156 – 1098 cm^{-1}. For IR spectral, the peak intensity was directly proportional with quantity (A); absorbance. The calculation of quantity ratio from IR spectral for determination of grafted MAH was based on absorbance rule that also been known as *Beer's* Law, which can be summarized in the following Equation 1:

$$A = -\log T = \log \frac{Io}{I} = \varepsilon lc \tag{1}$$

Where, ε is a molar absorbance, l is a sample thickness and c is a concentration value. Both ε and l can be obtained from the calibration curve of A versus c for all the prepared samples with known concentration value. For material analysis with presence of two components, ration method is used for quantitative analysis based on *Beer's* Law.

Referring to Equation (1), in the spectrum depicted in Figure 3, there are two-component presence whereby both component having its distinctive peak and not interfering between each other. Hence, it was assumed that the ration of quantities is not dependent on the thickness of the film, so the quantity ratio can be calculated by using the following Equation (2).

$$\frac{A1}{A2} = \frac{\varepsilon 1 C 1 l 1}{\varepsilon 2 C 2 l 2} = \frac{\varepsilon 1 C 1}{\varepsilon 2 C 2} \tag{2}$$

For material system with the presence of two components, the blend ratio was simplified as the Equation (3).

$$X_1 + X_2 = 1 \tag{3}$$

Hence, the quantity ratio is determined as the following Equation (4).

$$\frac{A1}{A2} = \frac{\varepsilon 1 x 1}{\varepsilon 2 x 2} = \frac{\varepsilon 1}{\varepsilon 2}\left(\frac{1}{X2} - 1\right) = -k + k\frac{1}{x2} \tag{4}$$

where, k is the molar absorbance and is given in the following Equation (5).

$$k = \frac{\varepsilon 1}{\varepsilon 2} \tag{5}$$

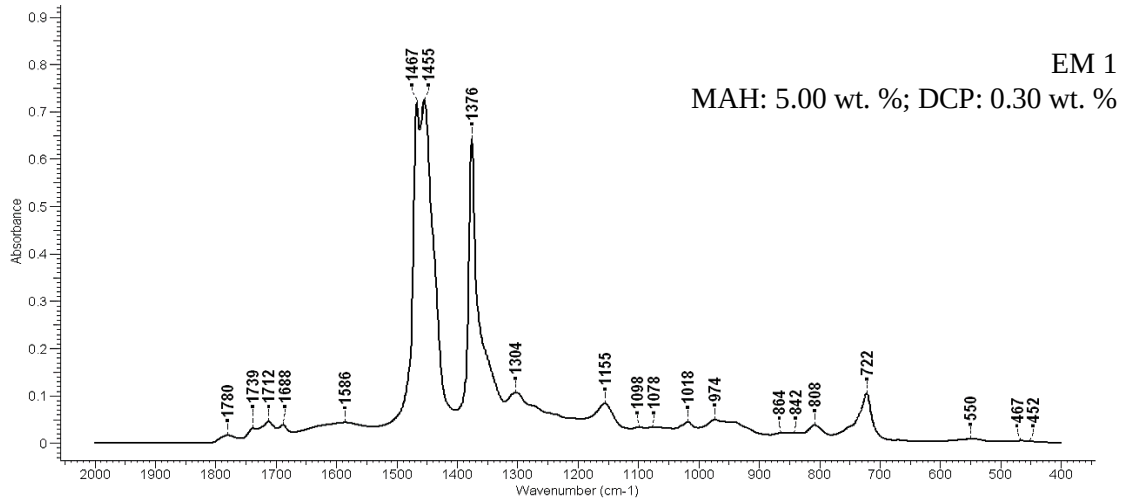

(a)

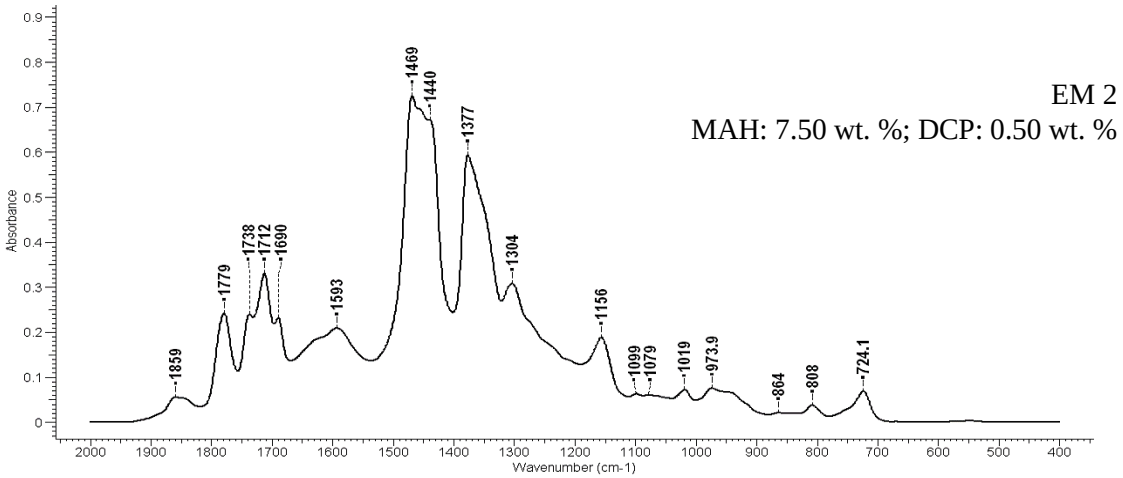

(b)

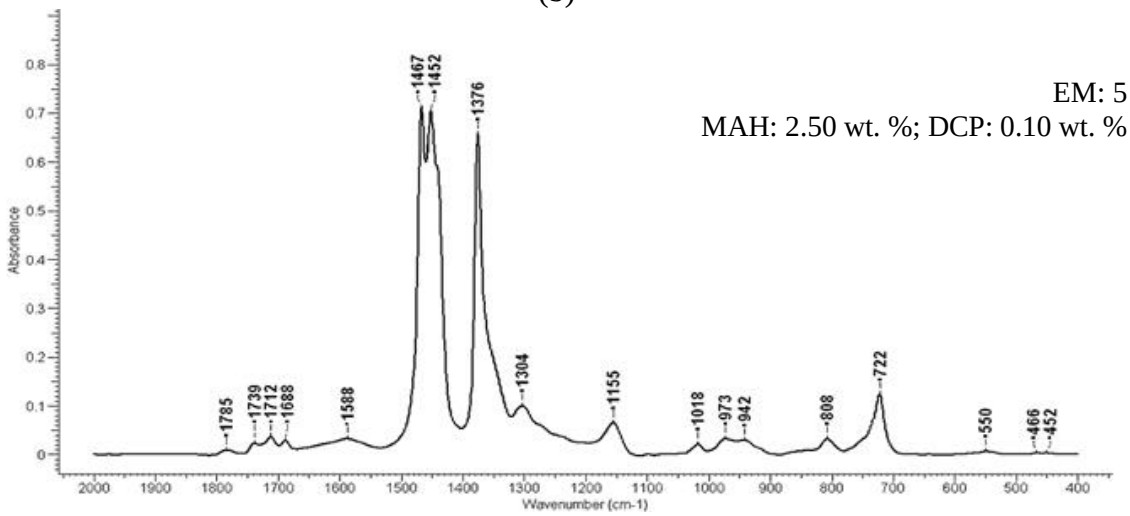

(c)

Figure 3. Selected IR spectral for grafted EPDM-*g*-MAH: (a) EM1, (b) EM2, (c) EM5.

In this study, peak at wavenumber 1466.60 cm^{-1} was selected as an internal standard after considering the consistent peak intensities at that particular wavenumber [16]. This peak is referred to the scissoring frequency for methylene, CH_2 in EPDM component. For quantity ratio calculation, the peak that represent C=O anhydride stretching at 1738.50 cm^{-1} is utilized. Standard calibration curve is plotted based on various MAH content (0, 2.50, 5.00 and 7.50 wt. %) and as presented as in the following Figure 4. The quantity ratio plots has exponentially increased with the MAH content. The calibration curve with MAH content function gives one exponent equation as in Equation 6 with R^2 value around 0.8919.

$$y = 0.0122e^{0.37266x} \tag{6}$$

$$\%\ MAH\ grafted\ into\ EPDM = \frac{1}{0.3726}\left(\ln\left[\frac{\frac{A1738.51cm^{-1}}{A1466.60cm^{-1}}}{0.0122}\right]\right) \tag{7}$$

The quantity of grafted MAH was then determined by using modified Equation 7 from the original Equation 6, considering the quantity ration for IR peak wavenumber range at 1738.50 and 1466.60 cm^{-1}. The percentage of grafted MAH was calculated and reported in the Table 3. Later, the normal half plot has generated by using the DOE software and depicted in the following Figure 5. From the half-normal plot, it was found that the variables A and B and interaction term of AB were deviated away from the straight plot line. No variables and interacting points are detected falls over the plot line. Based on this plot, both variables A (MAH content) and B (DCP content) are significant models.

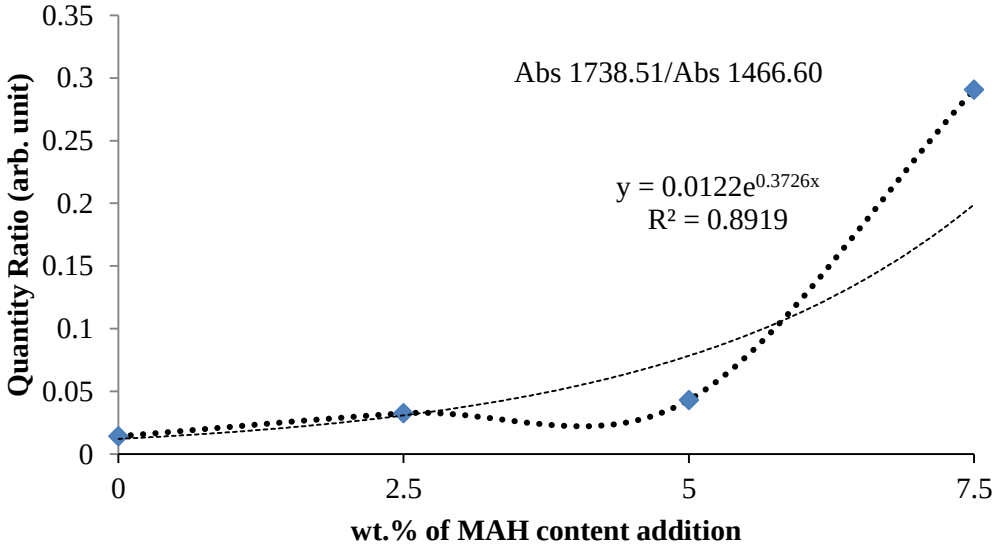

Figure 4. Standard calibration curve for EPDM-*g*-MAH for quantity ratio determination.

This decision has supported by a list of effects that indicate the numerical representation of each model terms, as in the Table 4. Variable B (DCP content) is the most significant factor with percentage of contribution about 67.45%. Interaction term of AB followed with 20.87% of contribution in the effect list. Both B and AB are positive value indicating that addition of A and B from low level into higher level, prone to increase the grafting efficiency of MAH.

DCP increased the radical formation during the grafting reaction that assisting the molecular chain movement into the rubber backbone [9]. ANOVA for quantity ratio determination as summarized in Table 5. Both variable of A and B are significant model terms with *p-value* less than 0.0500. The selected model has considered accurate and used to navigate the design analysis area with higher coefficient of determination, R^2. The selected model does not explain only 0.03% of total variation.

Table 3. Percentage of grafted MAH into EPDM calculated using absorbance ratio analysis.

	Factor 1	Factor 2	Internal Standard	Standard anhydride peak	
	A: MAH	*B*: DCP	1466.60 cm^{-1}	1738.51 cm^{-1}	Response
Sample	wt.%	wt.%	*arb. unit*	*arb. unit*	% grafting efficiency
Control	0	0	96.40	1.38	0.00
EM1	5.0	0.3	98.89	4.28	3.40
EM2	7.5	0.5	96.34	28.00	8.52
EM3	7.5	0.1	96.16	2.08	1.54
EM4	5.0	0.3	97.05	4.06	3.31
EM5	2.5	0.1	99.54	3.25	2.64
EM6	2.5	0.5	98.59	6.74	4.63
EM7	5.0	0.3	99.88	4.42	3.46

Table 4. Effect lists of each model term involved in EPDM-*g*-MAH grafting process.

Term	Studentised Effects	Total Square	% Contribution
A	1.39	1.95	6.53
B	4.48	20.12	67.45
AB	2.50	6.23	20.87

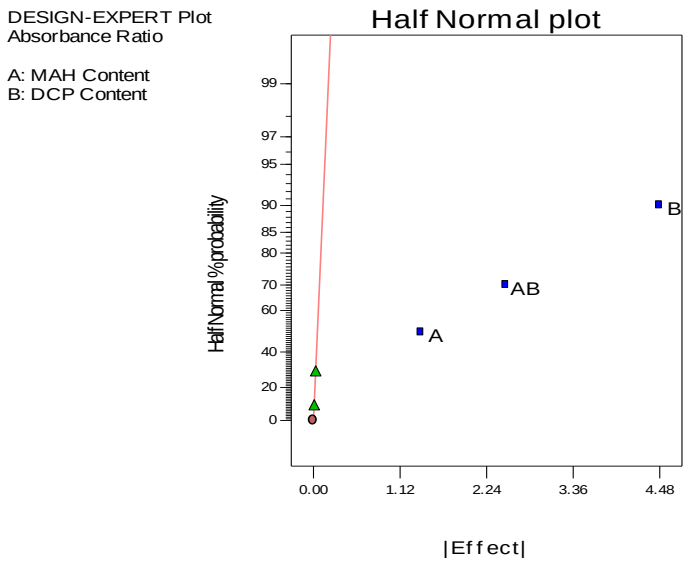

Figure 5. Half-normal plot of quantity ratio analysis for EPDM-*g*-MAH grafting efficiency studies.

Table 5. Analysis of variance for testing data utilizing the quantity ratio calculation.

Variation	Total of square	Degree of freedom	Average of square	F_o	*P-value*
Model	28.29	3	9.43	1654.17	0.0006
A	1.95	1	1.95	341.41	0.0029
B	20.12	1	20.12	3528.99	0.0003
AB	6.23	1	6.23	1092.11	0.0009
Curvature	1.52	1	1.52	267.16	0.0037
Error	0.011	2	5.6700e-003		
Total	18075.52	6			

Regression model for MAH grafting experiment is given in the following Equation 8. For this equation, variables A and B represented the MAH and DCP content, respectively. The note (+) at each level indicates both MAH and DCP are at the highest increment level. The regression coefficient +0.70 and +2.24 are one-half for the expected impact factor based on two-unit changes (from -1 to +1).

$$\text{Quantity Ratio} = + 4.33 + 0.70*A + 2.24*B + 1.25*A*B \quad (8)$$

Figure 8 presents a three dimensional plot for grafting efficiency response surface based on the selected model, with MAH and DCP content as the regresses coefficient. Based on the corresponding surface evaluation, it is clear that the grafting efficiency has increased with the increase of MAH and DCP content. The selection for the best strategy of EPDM-g-MAH grafting then implemented using the optimization menu available in the DOE software. The upper limit and the lower limit are considered to be within the range of 2.50 – 7.50 wt.% and 0.10 – 0.50 wt.% for MAH and DCP content, respectively. The grafting efficiency has been set to a maximum increase up to 8.52%. Re-experiment has found that the experimental

reproducibility generates only 9.30% of deviation value over the proposed output by the optimization tool.

Next, the success of EPDM-*g*-MAH grafting process then confirmed analytically by using a nuclear magnetic resonance (NMR) spectroscopy. Observation using NMR spectral helps in the proposed reaction mechanism of MAH grafting into EPDM rubber with DCP as initiator. Figure 7 and Figure 8 present the ^{1}H-NMR results for EPDM control sample and EPDM-g-MAH from optimum EM2 sample. Meanwhile, two-dimensional analysis results using 2D-COSY NMR spectra for both samples are shown in the following Figure 9 and Figure 10.

Referring to Figure 7, the presence of resonant signal at 0.8356 ppm showed the presence of CH_3 from the propyl group found on the EPDM backbone, while the resonant signal around 1.10 ppm showed the CH_2 on the EPDM and the signal around 2.0574 ppm was CH and CH_2 groups adjacent to olefin. The resonant signal at 4.9956 ppm was the vynilidene termination for EPDM, and the peak at 5.2310 ppm was the internal olefin of the diene on the terpolymer part. The EPDM aromatic part is shown as a weak resonant signal peat at 7.0 ppm. Grafting of MAH on the EPDM backbone has shifted some of the resonant signals found in the control sample with the presence of new peak detected at signal 4.00 ppm (Figure 8). The presence of new singlet from the peak of 4.00 ppm is the effect of *ene* reactions [17]. The absence of resonant at peak 6.50 ppm in the ^{1}H-NMR spectra for the EPDM-*g*-MAH sample and its control sample, explains that terpolymer MAH has been detected from this analysis [31-34].

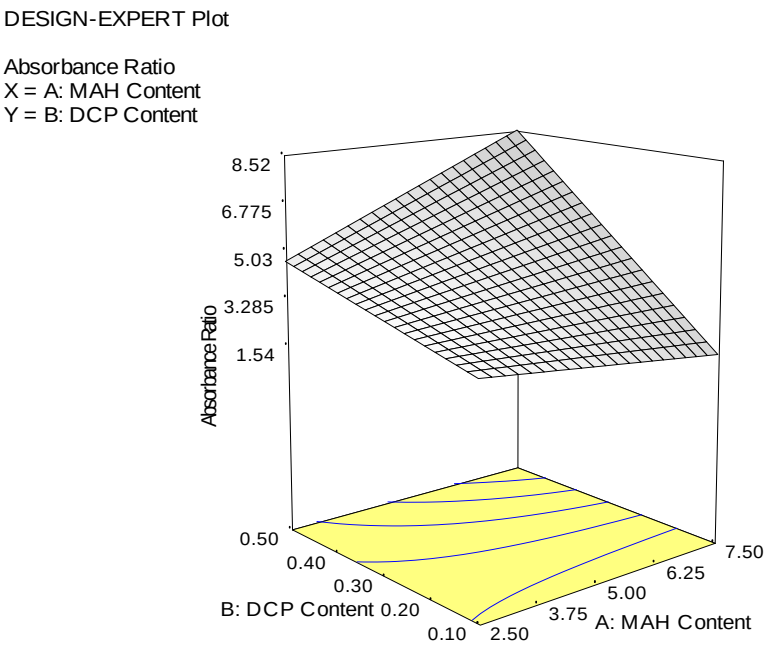

Figure 6. Response surface plot for MAH grafting efficiency using the quantity ratio approach.

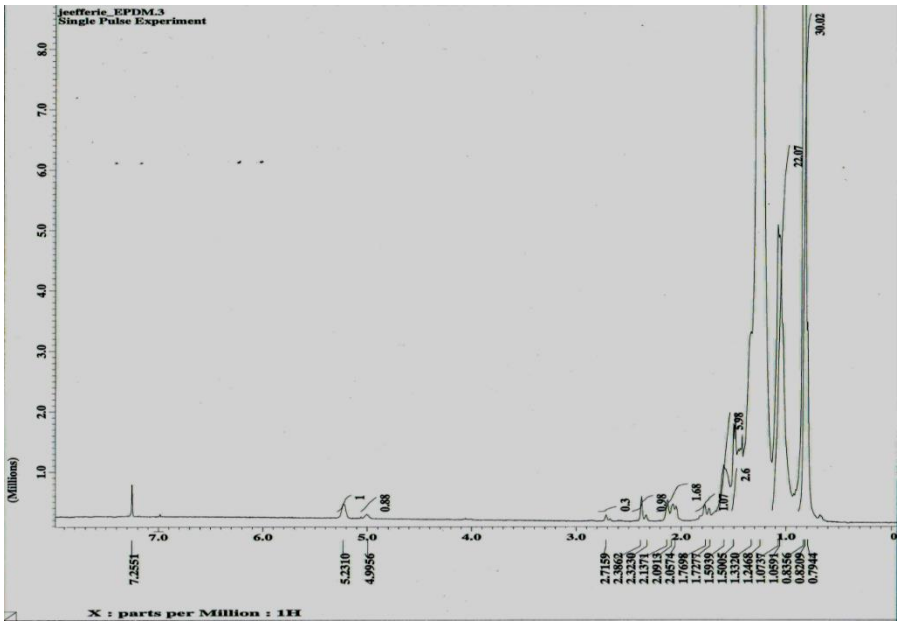

Figure 7. [1]H-NMR for pure EPDM rubber (control sample).

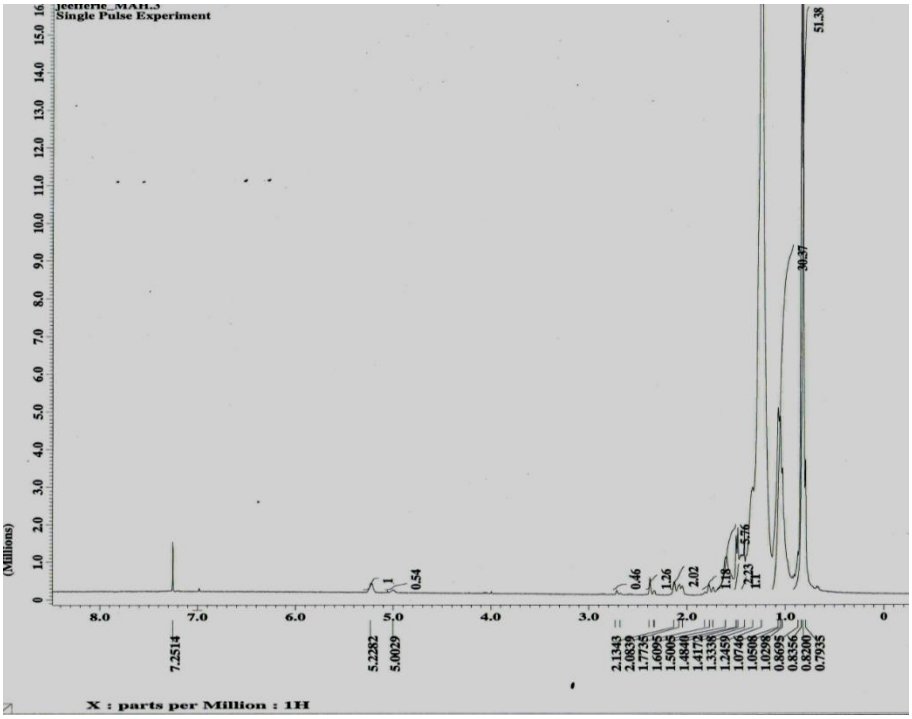

Figure 8. [1]H-NMR for grafted EPDM-*g*-MAH (EM2) sample.

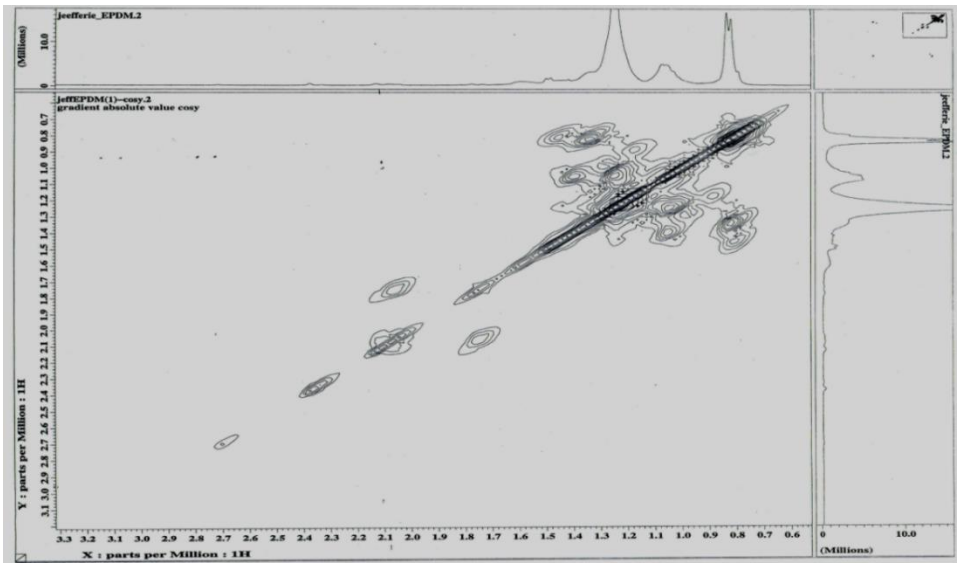

Figure 9. 2D-COSY for pure EPDM rubber (control sample).

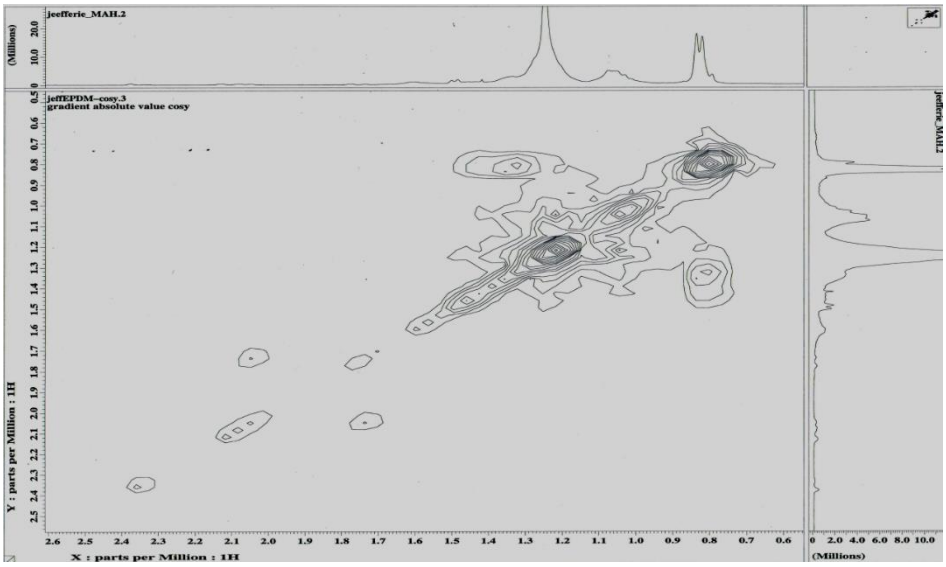

Figure 10. 2D-COSY for grafted EPDM-*g*-MAH (EM2) sample.

The grafting MAH reaction mechanism into EPDM visualized as in the following Figure 11. This reaction mechanism has supported by the ^{1}H-NMR and 2D-COSY NMR analysis as presented in the Figure 7 - 10. Those figures are original results that taken directly from the NMR machine and presence of noise and its background colour need to be ignore due to machine set-up, standard results and machine condition. The EPDM-g-MAH compatibilizer synthesized by using an internal mixer, which gives shearing effect that can help in breaking the chain [32, 33]. The presence of dicumyl peroxide initiator in very small quantities as shown in reaction schematic (1), has formed the start-up radical for reactive grafting reaction

of EPDM rubber. DCP radicals react with hydrogen atoms from the EPDM backbone to produce EPDM radicals as shown in the reaction scheme (2).

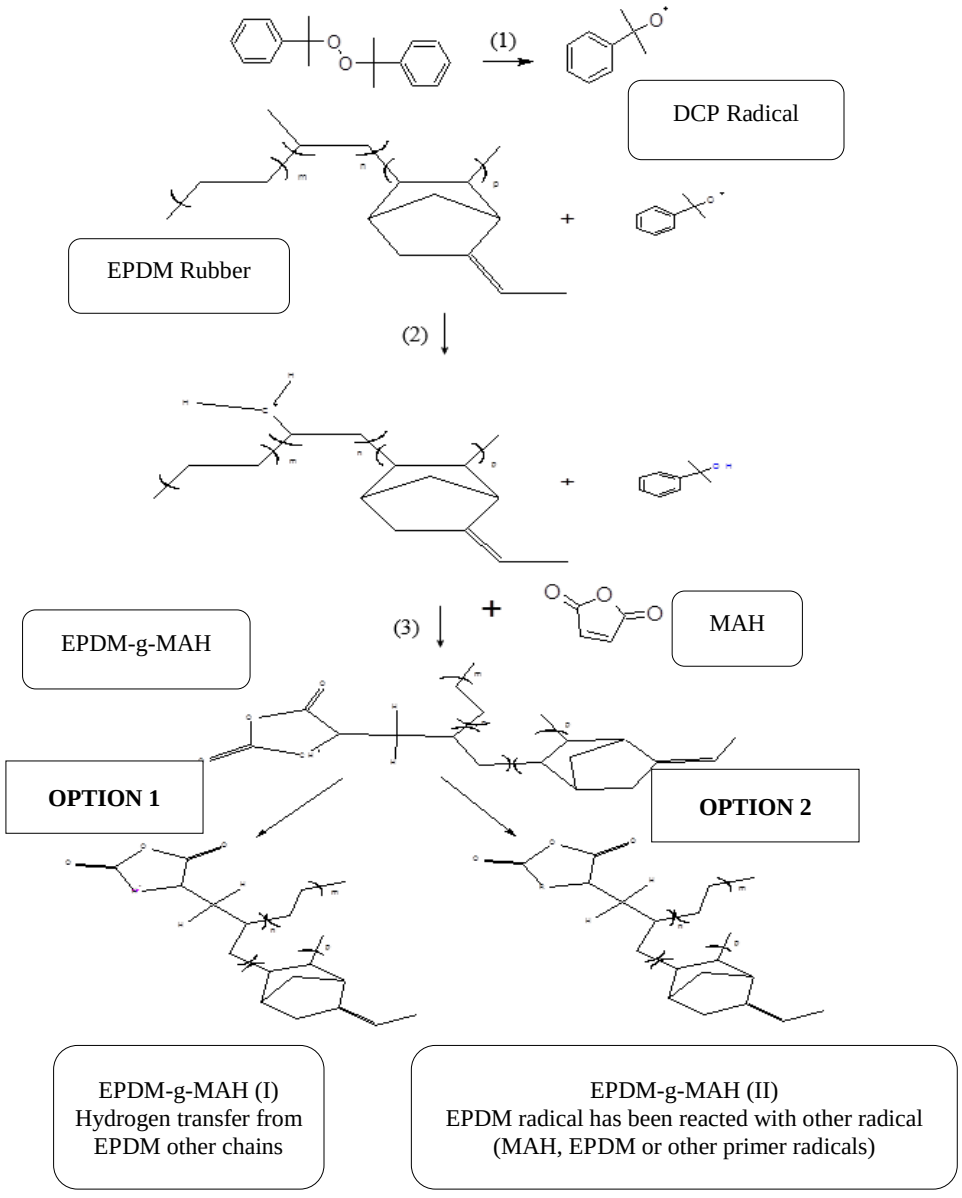

Figure 11. Proposed reaction mechanism model for EPDM grafting with MAH (EPDM-*g*-MAH).

The presence of DCP initiator in certain small quantity has helped in increasing the number of EPDM active radicals for the reaction with MAH. In the reaction schematic path (3), the MAH molecules added during the melt-blending were found to react with EPDM active radicals and grafting occurred in the formation of EPDM-*g*-MAH radicals, followed by several possibilities for termination reactions, based on two paths of reaction options [32, 33, 34]. Option (1) shows the EPDM-*g*-MAH radicals may undergo hydrogen transfer from other

polymer chains, whereas option (2) shows the possible radical reaction of EPDM-*g*-MAH with other radicals in the melt blending system such as MAH, EPDM or primary radicals to form different EPDM-*g*-MAH structures [9].

CONCLUSIONS

As a conclusion, preparation of EPDM-*g*-MAH compatibilizer in the laboratory scale using an internal mixer has successfully performed in this study, by applying a two level full factorial experimental design method with higher R^2 value of 99.97%. Interestingly, the MAH grafting efficiency was determined by applying the standard calibration curve and *Beers Lambert* absorbance law. 3D response surface curve has established the relationships between MAH and DCP content as independent variables towards the grafting efficiency response. Optimum grafting efficiency output up to 8.52% was obtained form 7.5 phr MAH and 0.50 phr DCP with about 67.45% of effects list has contributed solely by the DCP content factor. At the end, from the FTIR, ^{1}H-NMR and 2D-COSY spectral analysis has suggested that there are three (3) schematic reaction mechanism route with two (2) possible termination option for synthesizing the EPDM-*g*-MAH compatibilizer. This study provides the sustainability value on the possibility of EPDM-*g*-MAH compatibilizer development at the laboratory scale with higher yield and low cost requirements.

ACKNOWLEDGEMENTS

The authors would like to thank to the Universiti Teknikal Malaysia Melaka and Universiti Malaysia Pahang for laboratory facilities and financial assistance under UTeM Hi-Impact Short Term Research Grant (PJP/2016/FKP/H16/S01484) and UMP Fellowship Research Grant project No. RDU1703321.

REFERENCES

[1] Alipour A, Naderi G, Ghoreishy MH. Effect of nanoclay content and matrix composition on properties and stress-strain behavior of NR/EPDM nanocomposites. Journal of Applied Polymer Science. 2013;127(2):1275–1284.

[2] Ismail H, Mathialagan M. Comparative study on the effect of partial replacement of silica or calcium carbonate by bentonite on the properties of EPDM composites. Polymer Testing. 2012;31(2):199–208.

[3] Sadayuki N, Tatsuo S. Development of EPDM grades with good processability characteristics – specialized polymer design for anti-vibration rubber –. R&D Report, "Sumitomo Kagaku,". 2007;1.

[4] Mitra S, Ghanbari-Siahkali A, Kingshott P, Rehmeier HK, Abildgaard H, Almdal K. Chemical degradation of crosslinked ethylene-propylene-diene rubber in an acidic environment. Part I. Effect on accelerated sulphur crosslinks. Polymer Degradation and Stability. 2006;91:69-80.

[5] Arayapranee W, Rempel GL. Properties of NR/EPDM blends with or without methyl methacrylate-butadiene-styrene (MBS) as a compatibilizer. International Journal of Materials & Structural Reliability. 2007;5(1):1–12.
[6] Pasbakhsh P, Ismail H, Fauzi MNA, Bakar AA. Influence of maleic anhydride grafted ethylene propylene diene monomer (MAH-g-EPDM) on the properties of EPDM nanocomposites reinforced by halloysite nanotubes. Polymer Testing. 2009;28(5):548–559.
[7] Sae-oui P, Sirisinha C, Thepsuwan U, Thapthong P. Influence of accelerator type on properties of NR/EPDM blends. Polymer Testing. 2007;*26*(8):1062–1067.
[8] Zhang H, Datta RN, Talma AG, Noordermeer JWM. Maleic-anhydride grafted EPM as compatibilising agent in NR/BR/EPDM blends. European Polymer Journal. 2010;46(4):754–766.
[9] Phua YJ, Chow WS, Mohd Ishak ZA. Reactive processing of maleic anhydride-grafted poly(butylene succinate) and the compatibilizing effect on poly(butylene succinate) nanocomposites. Express Polymer Letters. 2013;*7*(4):340–354.
[10] Mangaraj D. Elastomer Blends. Rubber Chemistry and Technology. 2002; 75(3):365–427.
[11] El-Sabbagh SH. Compatibility study of natural rubber and ethylene-propylene diene rubber blends. Polymer Testing. 2003;22(1):93–100.
[12] Grigoryeva OP, Karger-Kocsis J. Melt grafting of maleic anhydride onto an ethylene–propylene–diene terpolymer (EPDM). European Polymer Journal. 2000;36(7):1419–1429.
[13] Matarredona O, Rhoads H, Li Z, Harwell JH, Balzano L, Resasco DE. Dispersion of single-walled carbon nanotubes in aqueous solutions of the anionic surfactant NaDDBS. The Journal of Physical Chemistry B. 2003;107(48):13357–13367.
[14] Nakason C, Kaesaman A, Samoh Z, Homsin S, Kiatkamjornwong S. Rheological properties of maleated natural rubber and natural rubber blends. Polymer Testing. 2002;21(4):449–455.
[15] Razak JA, Ahmad SH, Ratnam CT, Mahamood MA, Yaakub J, Mohamad N. Effects of EPDM-g-MAH compatibilizer and internal mixer processing parameters on the properties of NR/EPDM blends: An analysis using response surface methodology. Journal of Applied Polymers Science. 2015; 132:42199.
[16] Bellamy MK. Using FTIR-ATR spectroscopy to teach the internal standard method. Journal of Chemical Education. 2010;87(12):1399–1401.
[17] Vicente AI, Pereira SG, Nunes TG, Ribeiro MR. ^{1}H-NMR study of maleic anhydride modified ethylene-diene copolymers. Journal of Polymer Research. 2011;18(4):527–532.
[18] Razak JA, Mohamad N, Ab Maulod HE, Lau KT, Munawar RF, Abd Manaf ME, Ismail S, Mahamood MA. Characterization on thermal and mechanical properties of non-covalent polyethyleneimines wrapped on graphene nanoplatelets within NR/EPDM rubber blend nanocomposites. Journal of Advanced Manufacturing Technology. Special Issue (TMAC) Symposium. 2017:85–100.
[19] Liew PJ, Shaaroni A, Razak JA, Kasim MS, Sulaiman MA. Optimization of cutting condition in the turning of AISI D2 steel by using carbon nanofiber nanofluid. International Journal of Applied Engineering Research. 2017;12(10):2243–2252.

[20] Ashikur RKM, Rahman MM, Kadirgama K, Maleque MA, Ishak M. Prediction of surface roughness of Ti-6Al-4V in electrical discharge machining: A regression model. Journal of Mechanical Engineering and Sciences. 2011;1:16-24.
[21] Kaharuddin KE, Salehuddin F, Zain ASM, Abd Aziz MNI. Optimization of process parameter variations on leakage current in SOI vertical double gate MOSFET device. Journal of Mechanical Engineering and Sciences. 2016;1:1895–1907.
[22] Hanief M, Wani MF. Artificial neural network and regression-based models for prediction of surface roughness during turning of red brass (C23000). Journal of Mechanical Engineering and Sciences. 2016;1:1835–1845.
[23] Salehi S, Noaparast M, Shafaei SZ. Response surface methodology (RSM) for optimization of chalcopyrite concentrate leaching with silver-coated pyrite. Physicochemical Problems of Mineral Processing. 2016;52(2):1023–1035.
[24] Jamaluddin H, Ghani JA, Deros BM, Ab Rahman MN, Ramli R. Quality improvement using Taguchi method in shot blasting process. Journal of Mechanical Engineering and Sciences. 2016;2:2200–2213.
[25] Darestani NG, Tikka A, Fatehi P. Sulfonated lignin-g-styrene polymer: production and characterization. Polymers. 2018;10(198):1-17.
[26] Liu Z, Xu D, Xu L, Kong F, Wang S, Yang G. Preparation and characterization of softwood kraft lignin copolymers as a paper strength additive. Polymers. 2018;10(743):1–12.
[27] Zhou L, He H, Li MC, Huang S, Mei C, Wu Q. Grafting polycaprolactone diol onto cellulose nanocrystal via click chemistry: enhancing thermal stability and hydrophobic property. Carbohydrate Polymers. 2018.
[28] El-Hoshoudy AN, Desouky SM, Attia AM, Gomaa S. Synthesis and evaluation of xanthan-g-poly(acrylamide) co-polymer for enhanced oil recovery applications. Petroleum & Petrochemical Engineering Journal. 2018;2(3):1-8.
[29] Ku SG, Kim YC. Effect of grafting degree of maleic anhydride on the physical properties of expandable HDPE/KF. Annual International Conference on Chemical Processes, Ecology & Environmental Engineering (ICCPEE'16) April 28-29, 2016, Pattaya, Thailand.
[30] Koshy TM, Gowda DV, Tom S, Karunakar G, Srivastava A, Moin A. Polymer Grafting – An Overview. American Journal of Pharmtech Research. 2016;6(2):1-13.
[31] Adeniyi AT, Adekanmi DG. Characterization of native and graft copolymerized albizia gums and their application as a flocculant. Journal of Polymers. 2017; 3125385:1-9.
[32] Paoprasert P, Boonthong W, Kookarinrat C, Chantarasiri N. Preparation of stable polymeric grafted layers on poly(ethylene terephthalate) by thermal annealing. ScienceAsia. 2014;40(2014):224-231.
[33] Ahmad Zaki F, Abdullah I. Graft copolymerization of acrylonitrile onto torch ginger cellulose. Sains Malaysiana. 2015;44(6):853-859.
[34] Pandey VS, Shukla BK, Yadav M. Graft copolymer (guar gum-g-poly 2-acrylamidoglycolic acid): synthesis, swelling and flocculation behaviours. 2017;2(2):10-15.